

# Scattering Pattern Calculation for Large Finite Arrays using the Element-Varying Active Element Factor Method

Qifei Li, Wei Shao, and Hua Li

Institute of Applied Physics

University of Electronic Science and Technology of China, Chengdu, China

E-mail: qifei\_li@163.com, weishao@uestc.edu.cn, and lihua2006@uestc.edu.cn

**Abstract** — In this paper, an efficient approach for calculating the far field pattern of one-dimensional (1-D) and two-dimensional (2-D) finite patch arrays is proposed. Based on the active element factor (AEF) defined specifically for scattering problems, this proposed method takes into account the effects of mutual couplings and array edges. From the induced current distribution on an array with odd or even elements, the array is divided into different parts and neglects the weak mutual coupling affected by far elements for each part. Thus, the element-varying AEF method changes a large array problem into a superposition of various simplified subarray problems. Three examples verify the accuracy and efficiency of the proposed method. Furthermore, the results show that the proposed method with the element-varying AEF technique has the ability to solve the scattering problems of rather large arrays whereas other methods become incapable due to computer hardware limitations.

**Index Terms** — Active element factor, far field pattern, mutual coupling, subarray.

## I. INTRODUCTION

Numerical methods, such as the method of moments (MoM) [1], finite element method (FEM) [2], finite-difference time-domain (FDTD) method [3], multilevel fast multipole algorithm (MLFMA) [4], characteristic basis function method (CBFM) [5], and hybrid methods [6] are employed to calculate the electromagnetic scattering. Direct numerical simulations for a small array mounted on an arbitrary platform result in an accurate and effective solution. For an infinite periodic array, only an element is required to be extracted for calculation with the Floquet's

theorem or periodic Green function [7-8]. The numerical methods, however, become inefficient or even infeasible for rather large finite arrays when considering the mutual coupling effects in the whole array environment because of the computer hardware limitations. In this case, approximate methods are needed to reduce the large memory and time requirement for the array calculation and analysis.

Over the past years, an active element pattern (AEP) technique was used for prediction of the performance of large array antennas [9-11]. With the pattern taken with a feed at a single element in the array and all other elements terminated in matched loads, the AEP technique considers mutual coupling effects between array elements and expresses the radiated pattern effectively and efficiently. From the AEP theorem, the active element factor (AEF) defined as the current distribution induced on a particular aperture is intended for scattering problems [12-13]. In [13], an average AEF with the reduced window array (RWA) approximation is introduced to analyze the scattering characteristics of finite arrays in an infinite ground plane.

In this paper, the scattering performance of finite patch arrays in a finite ground plane is studied with an element-varying AEF method. Due to the finite grounds in this study, the induced current distribution on an array with odd elements is quite different from that with even elements. Based on the element-varying AEF method, this paper presents how an array is divided into various subarrays according to the induced current distribution. The whole array elements are divided into edge elements, interior elements, and adjacent edge elements. The AEFs of edge elements can be approximated by a small subarray when neglecting

the weak mutual coupling affected by far elements. The similar subarrays are also applied to AEFs of interior elements and adjacent edge elements. Thus, the far field pattern of a rather large finite array can be calculated by a superposition of these three types of the element-varying AEF from a subarray. After the current distribution of a small array is quickly gotten with the commercial software FEKO [14], the varied AEFs of each element in a subarray can easily be obtained to calculate the far field scattering pattern of a rather large array. The element-varying AEF method can greatly reduce the computing time and simplify the operational procedure. The one-dimensional (1-D) and two-dimensional (2-D) examples show that the results are actually quite good over a broad angular range and only deteriorate for angles that approach grazing.

## II. THEORIES

### A. Far electric field pattern of a finite array

The far electric field scattered by an array can be expressed as

$$\mathbf{E}_{\text{total}} = \sum_{n=1}^N \mathbf{E}_n(\theta, \varphi), \quad (1)$$

where  $\mathbf{E}_n$  is the far electric field scattered by the  $n$ th element aperture with an entire array illuminated by an incident wave source. Induced currents on each element aperture are excited by the incident wave and contain all the effects of the mutual coupling and the array environment. Using the equivalence principle,  $\mathbf{E}_n$  can be written as

$$\begin{aligned} \mathbf{E}_n(\mathbf{J}, \mathbf{M}) = & -\frac{j\omega\mu}{4\pi} \int_s \mathbf{J} \frac{e^{-jk|\mathbf{r}-\mathbf{r}'|}}{|\mathbf{r}-\mathbf{r}'|} ds' \\ & + \frac{1}{4\pi j\omega\epsilon} \nabla \int_s \nabla' \cdot \mathbf{J} \frac{e^{-jk|\mathbf{r}-\mathbf{r}'|}}{|\mathbf{r}-\mathbf{r}'|} ds', \quad (2) \\ & -\frac{1}{4\pi} \nabla \times \int_s \mathbf{M} \frac{e^{-jk|\mathbf{r}-\mathbf{r}'|}}{|\mathbf{r}-\mathbf{r}'|} ds' \end{aligned}$$

where  $\mathbf{r}$  and  $\mathbf{r}'$  are the position vectors of the observation and source points with respect to a global coordinate, the electric current  $\mathbf{J}$  consists of  $\mathbf{J}_c$  and  $\mathbf{J}_d$  which are the equivalent surface electric currents induced on the conducting and dielectric surfaces of the  $n$ th element aperture, and the magnetic current  $\mathbf{M}$  is the equivalent surface magnetic current induced on the dielectric surface of the  $n$ th element aperture.

In this study,  $\mathbf{J}_c$ ,  $\mathbf{J}_d$  and  $\mathbf{M}$  can be gotten with the commercial software FEKO, which is a powerful and convenient tool. The current information is stored in \*.os file and mesh information in \*.stl file after the MoM-based simulation of FEKO. Thus,  $\mathbf{E}_n$  can be easily calculated by applying the corresponding current and mesh data to equation (2).

### B. Element-varying AEF method

Figure 1 plots a 1-D homogeneous finite periodic array illuminated by a plane wave source. Currents are induced on the structure. Besides the mutual couple effects, there are edge effects introduced by the bounded nature of the finite array [15-16]. Since the currents induced on each element are varied, all  $\mathbf{E}_n$  are needed to be calculated from (2) to complete the superposition of all elements' scattering patterns in (1).



● Edge      ● Adjacent edge      ○ Interior

Fig. 1. 1-D finite periodic array and its elements.

Considering the element-varying AEF scheme, a fast approximation is proposed to obtain the accurate scattering performance in this paper. Once knowing the currents induced on a small array with the numerical simulation, the far field pattern of a rather large finite array can be easily calculated.

Generally, all elements of an array are divided into edge elements, interior elements, and adjacent edge elements, as shown in Figure 1. Equation (1) can therefore be rewritten as [16]

$$\mathbf{E}_{\text{total}} = \mathbf{E}_E(\theta, \varphi) + \mathbf{E}_I(\theta, \varphi) + \mathbf{E}_{AE}(\theta, \varphi), \quad (3)$$

$$\mathbf{E}_E = \sum_{e=1}^{N_e} \mathbf{E}_e(\theta, \varphi) e^{jk\hat{\mathbf{r}} \cdot \mathbf{r}_e}, \quad (4)$$

$$\mathbf{E}_I = \sum_{i=1}^{N_i} \mathbf{E}_i(\theta, \varphi) e^{jk\hat{\mathbf{r}} \cdot \mathbf{r}_i}, \quad (5)$$

$$\mathbf{E}_{AE} = \sum_{a=1}^{N_a} \mathbf{E}_a(\theta, \varphi) e^{jk\hat{\mathbf{r}} \cdot \mathbf{r}_a}, \quad (6)$$

where  $\mathbf{E}_E$ ,  $\mathbf{E}_I$  and  $\mathbf{E}_{AE}$  are the superposition of AEP of all edge elements, all interior elements and all adjacent edge elements, respectively.  $N_e$ ,  $N_i$

and  $N_a$  are the numbers of all edge elements, all interior elements and all adjacent edge elements, respectively.  $E_e(\theta, \varphi)$ ,  $E_i(\theta, \varphi)$  and  $E_a(\theta, \varphi)$  are obtained from the local subarrays, respectively.

$e^{jk\hat{r}\cdot\mathbf{r}_e}$  is the spatial phase factor, where  $\hat{r}$  is the unit radius vector from the origin to the observation, and  $\mathbf{r}_n$  ( $n=e, i, a$ ) is a position vector from the origin to the center of the  $n$ th element.

### C. Arrays with odd and even elements

In the light of boundary condition and symmetry influence, the induced current distribution on an array with odd elements is quite different from that with even elements. In order to calculate AEFs of a rather large array from those of a small array accurately, it is required to calculate the two cases of odd elements and even elements, separately.

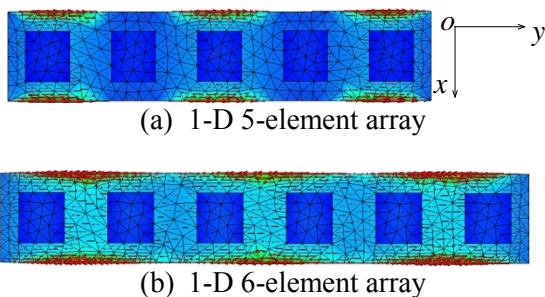


Fig. 2. Current density on odd-element and even-element arrays. (Arrows denote current densities.)

For example, Fig. 2 shows the induced current density on two finite patch arrays with five (odd) elements and six (even) elements from the FEKO simulation. The elements of the 1-D patch array are uniformly placed along the  $y$ -axis. And the two arrays are respectively illuminated by a vertical incident plane wave with  $y$  polarization. For the two cases, the symmetrical structure and the vertical plane wave source result in a symmetrical induced current distribution. However, the symmetry line along the  $y$ -direction of the odd-element array passes through one patch, but it is between two patches for the even-element array. The two different boundary conditions lead to the separate analysis of the odd-element array and even-element array. From Fig. 2, it can be seen that the current density on the array with odd elements is quite different from that with even elements.

## III. EXAMPLES AND DISCUSSIONS

### A. Far field calculation for 1-D arrays

In this section, various results are obtained by using the formulation presented in Section II. A 10-element period structure illuminated by a plane wave with  $\theta_0 = 0$  and  $\varphi_0 = 90$  is shown in Fig. 3. Each patch dimension is chosen to be  $w \times l$  ( $w=55.5\text{mm}$ ,  $l=60.6\text{mm}$ ). The thickness of the substrate  $h=0.762\text{mm}$  and relative permittivity is chosen as  $\epsilon_r=1.0$  for simplicity. Each element is uniformly spaced from its neighbors by a distance of  $d=0.51\lambda_0$  in the  $y$ -direction. The central operating frequency is 1.42GHz.

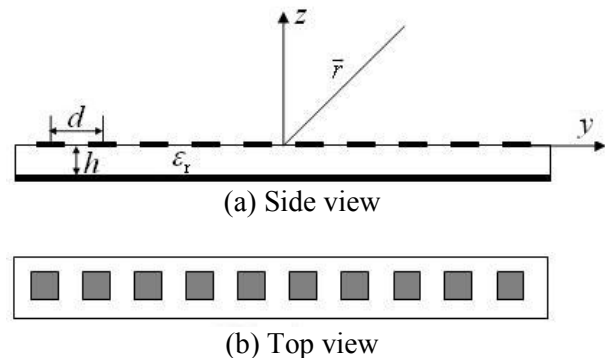


Fig. 3. A 1-D 10-element array.

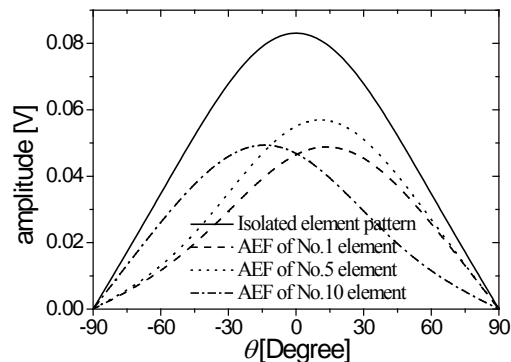


Fig. 4. Patterns calculated with isolated element and AEFs.

Figure 4 shows the isolated element pattern and varied AEFs involving all elements. It is clear that the isolated element pattern is different from the pattern of the AEFs because of the mutual-coupling effects.

The following is to determine the number of elements in a subarray involved to calculate AEFs of edge elements, adjacent edge elements and

interior elements. Firstly, the far field pattern of left edge element is investigated. Figure 5 shows the far field pattern in the E-plane of left edge element in the subarray. The left edge pattern of the 4-element subarray is almost coinciding with that of the 6-element subarray. Therefore, the left edge element pattern can be determined by a 4-element subarray. Secondly, the far field pattern of the left adjacent element can be determined by a 6-element subarray from Fig. 6. Thirdly, the far field pattern of the odd interior element can be obtained by a 6-element subarray from Fig. 7. The elements on the right side can be treated in a similar way.

Therefore, only a 6-element subarray is involved to obtain all three kinds of AEF for the even-element arrays no matter how large the total element number is.

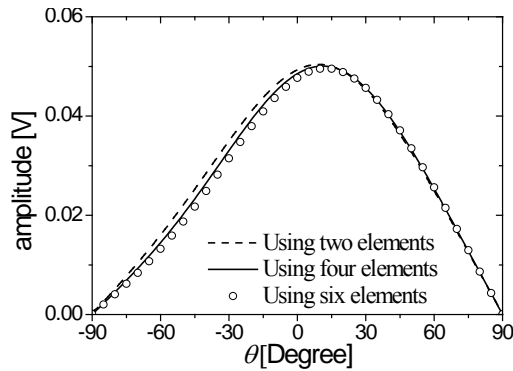


Fig. 5. AEFs of the left edge element by using different subarrays.

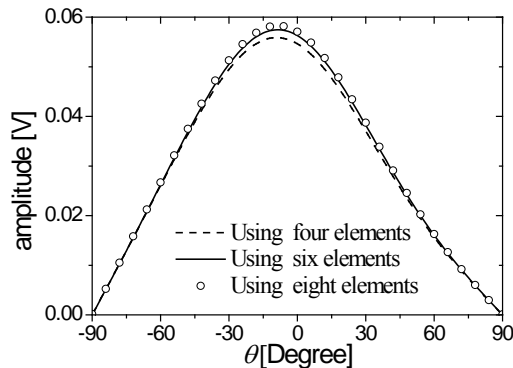


Fig. 6. AEFs of the left adjacent element by using different subarrays.

Based on the 6-element subarray, Fig. 8 plots the far field patterns of a 1-D 10-element patch array using the element-varying AEF method and

the whole-array simulation with FEKO, respectively.

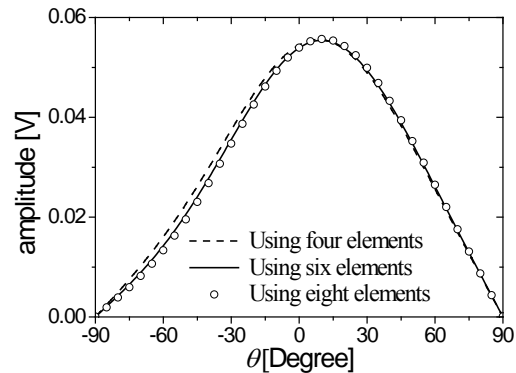


Fig. 7. AEFs of the odd interior element by using different subarrays.

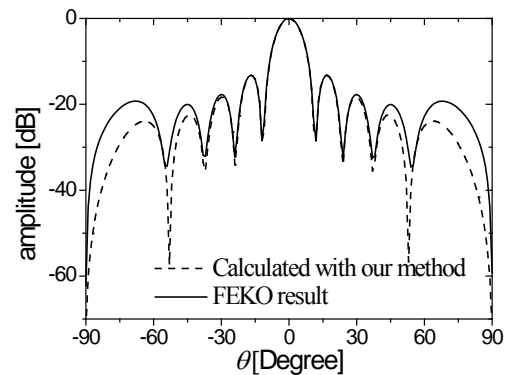


Fig. 8. Far-field pattern for the 1-D 10-element array.

The same analysis applies to an array with odd elements. Only a 5-element subarray is required to calculate the far field scattering of rather large odd-element arrays. Figure 9 plots the far field patterns of a 1-D 51-element patch array. The results show that the pattern with the element-varying AEFs method closely matches that with the whole-array simulation.

Table 1 presents the computing time comparison between the proposed method and the whole-array simulation with FEKO for the studied arrays. The proposed method shows a significant improvement in computational efficiency. All calculations are performed with an Intel Pentium Dual-Core 2.93GHz computer having 2.0GB of RAM.

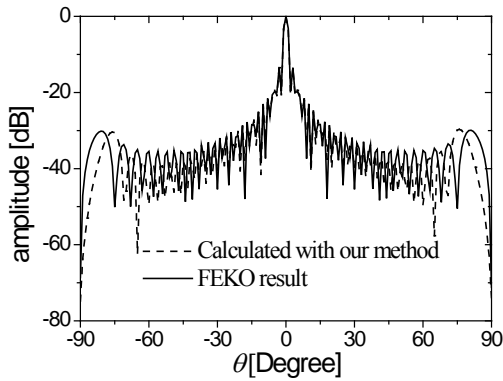


Fig. 9. Far-field pattern for the 1-D 51-element array by FEKO's simulation and the element-varying AEFs method.

Table 1: A comparison of the computing time between our method and the 1-D whole-array simulation with FEKO

10-element array	Our method	FEKO
Subarray simulation (s)	1.78	—
AEP superposition (s)	$0.07 \times 10^{-2}$	—
Total time (s)	1.78	4.45
51-element array	Our method	FEKO
Subarray simulation (s)	1.22	—
AEP superposition (s)	0.01	—
Total time (s)	1.23	153.75

### C. Far field calculation of 2-D finite array

The geometry of a 2-D  $5 \times 5$  array illuminated by a plane wave with  $\theta_0 = 0$  and  $\varphi_0 = 90$  is shown in Figure 10. The materials and patch sizes are the same as the 1-D cases. Similar to a 1-D array, the array elements can be divided into corner elements, edge elements and interior elements. The analysis procedure is the same as that for a 1-D array. Thus, only a  $5 \times 5$ -element subarray is required to calculate a 2-D rather large odd-element array. Figure 11 illustrates the far field patterns for a 2-D  $11 \times 11$ -element array using the element-varying AEF method and the whole-array simulation with FEKO.

Table 2 shows that the proposed method for the 2-D  $11 \times 11$ -element array gets a significant improvement in computational efficiency compared to the whole-array simulation.

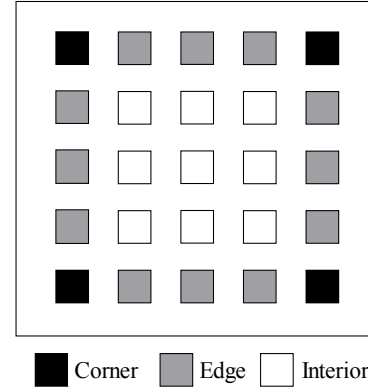


Fig. 10. Geometry of a 2-D  $5 \times 5$ -element array and its elements.

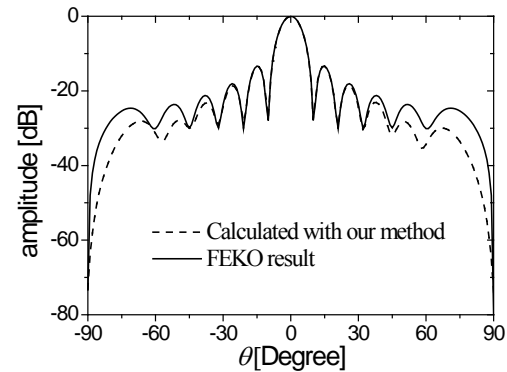


Fig. 11. Far-field pattern for an  $11 \times 11$ -element array.

Table 2: A comparison of the computing time between our method and the whole-array simulation with FEKO

	Our method	FEKO
Subarray simulation (s)	39.14	—
AEP superposition (s)	0.15	—
Total time (s)	39.29	10254.05

## VI. CONCLUSION

In this paper, we introduce a convenient and efficient method for calculating the far field pattern of finite periodic arrays. The element-varying AEF method, considering the effects of mutual coupling and edge surroundings, involves the edge, adjacent and interior element factor patterns. Thus, it merely needs to simulate a small subarray to obtain the scattering pattern of rather large arrays. The numerical examples show that the proposed method is valid and efficient for calculating the far field scattering pattern.

## ACKNOWLEDGMENT

This work is supported in part by the National Natural Science Foundation of China (60901023), the DPR Foundation (9140A03011210DZ02) and the Fundamental Research Funds for the Central Universities (ZYGX2010J043).

## REFERENCES

- [1] R. F. Harrington, *Field Computation by Moment Methods*, Macmillan, New York, 1968.
- [2] J. M. Jin, *The Finite Element Method in Electromagnetics*, Wiley, New York, 1993.
- [3] A. Taflove and S. C. Hagness, *Computational Electrodynamics: The Finite-Difference Time-Domain Method*, Artech House, 2000.
- [4] H. Fangjing, N. Zaiping, and H. Jun, "An Efficient Parallel Multilevel Fast Multipole Algorithm for Large-scale Scattering Problems," *Applied Computational Electromagnetics Society (ACES) Journal*, vol. 25, no. 4, pp. 381-387, 2010.
- [5] R. Maaskant, R. Mittra, and A. Tjihuis, "Fast Solution of Multi-Scale Antenna Problems for the Square Kilometre Array (SKA) Radio Telescope Using the Characteristic Basis Function Method (CBFM)," *Applied Computational Electromagnetics Society (ACES) Journal*, vol. 24, no. 2, pp. 174-188, 2009.
- [6] S. Y. He, C. Li, F. Zhang, G. Q. Zhu, W. D. Hu, and W. X. Yu, "An Improved MM-PO Method with UV Technique for Scattering from an Electrically Large Ship on a Rough Sea Surface at Low Grazing Angle," *Applied Computational Electromagnetics Society (ACES) Journal*, vol. 26, no. 2, pp. 87-95, 2011.
- [7] F. Xu, Y. L. Zhang, W. Hong, K. Wu, and T. j. Cui, "Finite-Difference Frequency-Domain Algorithm for Modeling Guided-wave Properties of Substrate Integrated Waveguide," *IEEE Trans. Microwave Theory Tech.*, vol. MTT-51, pp. 2221-2227, 2003.
- [8] S. Singh, J. R. Zinecker, and D. R. Wilton, "Accelerating the Convergence of Series Representing the Free Space Periodic Green's Function," *IEEE Trans. Antennas and Propagat.*, vol. AP-38, pp.1958-1962, 1990.
- [9] D. M. Pozar, "The Active Element Pattern," *IEEE Trans. Antennas and Propagat.*, vol. AP-42, pp. 1176-1178, 1994.
- [10] D. M. Pozar, "A Relation between the Active Input Impedance and the Active Element Pattern of a Phased Array," *IEEE Trans. Antennas and Propagat.*, vol. AP-51, pp. 2486-2489, 2003.
- [11] D. F. Kelley and W. L. Stutzman, "Array Antenna Pattern Modeling Methods that Include Mutual Coupling Effects," *IEEE Trans. Antennas and Propagat.*, vol. AP-41, pp. 1625-1632, 1993.
- [12] F. J. Villegas, Y. Rahmat-Samii, and D. R. Jackson, "The Characteristics of Scattering from Finite Arrays of Nonuniform Cylindrical Cavities in a Ground Plane," *IEEE APS Int. Symp. Dig.*, Boston, MA, pp. 746-749, 2001.
- [13] F. J. Villegas, Y. Rahmat-Samii, and D. R. Jackson, "Scattering Characteristics of Finite Arrays of Cylindrical Cavities in an Infinite Ground Plane," *IEEE Trans. Antennas and Propagat.*, vol. AP-51, pp. 2369-2379, 2003.
- [14] FEKO, ver. 5.2, EM Software & System-S. A. (Pty) Ltd., Available: <http://www.feko.info>.
- [15] D. M. Pozar, "Finite Phased Arrays of Rectangular Microstrip Patches," *IEEE Trans. Antennas and Propagat.*, vol. AP-34, pp.658-665, 1986.
- [16] Q. Q. He, B. Z. Wang, and W. Shao, "Radiation Pattern Calculation for Arbitrary Conformal Arrays that Include Mutual-Coupling Effects," *IEEE Antennas and Propagat. Magazine*, vol. 52, pp. 57-63, 2010.



Qifei Li received the B.E. degree in Chengdu University of Information Technology, Chengdu, China, in 2006. From 2009 to now, she is pursuing the M.Sc. degree in the Institute of Applied Physics at the University of Electronic Science and Technology of China (UESTC), Chengdu, China. Her current research interests include the antenna radiation and array scattering.



**Wei Shao** received the M.Sc. and Ph.D. degrees in Radio Physics from UESTC, Chengdu, China, in 2004 and 2006, respectively.

He joined the UESTC and is now an associate professor. He has been a Visiting Scholar in the Electromagnetic Communication Laboratory, Pennsylvania State University in 2010. His research interests include the computational electromagnetics and antenna technique.



**Hua Li** received the Ph. D. degrees in Radio Physics from UESTC, Chengdu, China, in 2011. She joined the UESTC in 2002 and is currently a lecturer there. Her current research interests are in the areas of antenna technique and electromagnetic scattering.